IMPACT OF THE TEMPERATURE GRADIENT BETWEEN TWIN INCLINED JETS AND AN ONCMOING CROSSFLOW ON THEIR RESULTING HEAT TRANSFER

Amina Radhouane[1*], Nejla Mahjoub[1], Hatem Mhiri[1], George Le Palec[2] and Philippe Bournot[2]
[1] Unité de thermique et de thermodynamique des procédés industriels
Ecole Nationale d'Ingénieurs de Monastir, Route de Ouardanine, 5000 Monastir, Tunisie
[2] IUSTI, UMR 6595, Technopôle Château-Gombert, 5 rue Enrico Fermi
13013 Marseille, Cedex 20, France
([*] Corresponding author: radhouane_amina@yahoo.fr)

ABSTRACT. This paper deals with the interaction of twin inclined jets in crossflow. The consideration of this particular configuration is of great interest due to its wide presence in various domains and applications and to its dependence in many parameters. These parameters may be geometric like the jets' height, the jet nozzles' separating distance, the jet nozzles, exit section, etc... It may also be based upon one of the reigning features like the velocity ratio, the temperature gradient, etc…the gradient between the jets and the crossflow temperatures is precisely the parameter we intend to handle in the present work due to its great relevance in several environmental concerns and in technical constraints as well. The evaluation of this parameter will be carried out numerically on the temperature distribution itself. This evaluation is likely to give a thorough idea about the cooling/heating process resulted from the jets' interaction with the oncoming crossflow. Such an understanding is likely to give viable solutions to problems raised by this configuration like the acid rain engendered by too hot fumes or the deterioration of the combustors' walls by too high temperature jets, etc…
The numerically simulated model is based on the resolution of the Navier-Stokes equations by means of the finite volume method and the RSM second order turbulent model and is validated by confrontation to experimental data depicted on the same geometric replica.

INTRODUCTION

"Twin jets in crossflow" is a common configuration present in various industrial and academic domains. The number of applications where we find it is in constant increase and the chimney stack exhaust is for sure the most familiar one. Nevertheless, further typical engineering applications make reference to this configuration like the aerodynamics of VSTOL aircrafts and the jet steering systems, the combustion and chemical chamber mixing, etc…
In the literature, the interest was rather paid to single and multiple jets in crossflow but too few works were dedicated to the intermediate twin jets' configuration. Its well understanding is on the contrary very important in the way it expresses the transition between both of them with all it contains in terms of newly developed features or in the contrary of disappearing ones. Ziegler et al.[1970] are pioneer in the domain as they considered the question since the early seventies (1970) by examining a double jet emitted normally in both tandem and side by side arrangements towards the mainstream. This primer work was based upon a physical model that was validated after confrontation to experimental data relative to two jets injected normal and at 60º to the cross flow. It was shown through this work the effect of each of the jets on each others as well as the higher deflection of the upstream jet by the mainstream; the deflection process being actually originated from both the entrainment of the

mainstream fluid and of the pressure forces acting on the boundary of each jet. Di Micco et al. [1990(a)] adopted the same procedure as they considered twin jets in crossflow in both arrangements: tandem and side by side. This work was experimental as it was carried out by means of flow visualizations and aimed at examining the progression and mixing processes under the variation of the jet nozzles' spacing and the momentum flux ratio. Qualitative information was drawn from these observations like the penetration of both jets that proved to be low under the reduction of both of the tested parameters. When they increase, the penetration of the jet structures on the contrary grew and reached approximately 5 percent of the single jet case. A second part of this work allowed Di Micco et al. [1990(b)] to test the influence of a further parameter: the jets spacing to diameter ratio that ranged from 2.7 to 12.1. This influence was tested on the depth penetration of the jets that was proved to me non significant under a variable angular orientation. It was also tested on the type of interference between the interacting flows since the latter proved to constructive under the lowest spacing and both constructive and destructive for all the remaining values always under a variable angular orientation.
The most recent work dealing similarly with the twin jet in crossflow configuration is that of Kolar et al. [2006] as it experimentally considered the same arrangements. Attention is however exclusively dedicated to laterally oriented jets. This work is actually an extension of previous results relative to a single jet configuration and aim essentially to explore the vorticity distribution and the overall circulation associated with the dominant vortical structure of the handled double jet configuration. These features proved to be globally similar to the well-known contrarotating vortex pair of the single jet in crossflow.

Further authors chose to consider the twin jets in crossflow by comparing its behavior to the single jet case. Such a procedure was initiated by Moore et al. [1985] and aimed precisely to examining the interaction between engine exhaust jets and the freestream due to their great relevance on the aerodynamic and stability characteristics of VTOL aircrafts during the transition from hover to forward flight. The meant interactions are actually investigated by testing the influence of a non uniform velocity profiles on the surface pressure distribution due to their close relationship. Different injection ratios were also tested which allowed concluding that a non uniform jet with a high velocity periphery and a low velocity core has a higher effective velocity ratio than a uniform jet with the same mass flow. An experimental examination carried by Toy et al. [1992] established a similar rapprochement between the twin and single normal jets in crossflow by focusing on the interface region interactions. Smoke flow visualizations and a quantitative video digital imaging were combined to obtain the needed measurements relatively to both inline and side by side arrangements. The obtained data demonstrated the similarity of the growth rates in the downstream direction of both the mixing region and the half-width (defined by the mean interface location). A further spectral examination of the lateral fluctuations of the interface in each downstream plane across the jets showed the transfer in almost all cases of the energy from lower to higher frequencies with increasing distances from the wall. Kolar et al. [2007] paid recently a similar attention to the interactions between tandem and side by side twin jets in crossflow in order to detail the resulting mixing and dispersion processes. A particular emphasis was however put on the new velocity-field analysis based on kinematic decomposition techniques and a particular attention was dedicated to the large-scale vortical structures as well as to the background turbulence. This work could essentially delimitate the similarities and differences between the dominant mean-flow vortical features, vorticity and circulation associated with considered arrangements, establish a comparison with the single jet case and finally discuss some dispersion aspects that were reflected through the concentration measurements of the differently arranged twin buoyant stack plumes.

Other researchers chose to compare the double jets' configuration rather to both the single and the multiple jets in crossflow configurations. The first to having done this are Ziegler et al. [1973].

Procedures were developed for the matter and could provide a good characterization of the jets' progression among the crossflow by means of the velocity stratification. Jets with three different types of exit velocity stratification have been considered, namely: jets with a relatively high velocity core, jets with a relatively low velocity core and jets originating from a vaned nozzle. They even were tested in different arrangements: tandem, side by side and not aligned. In each case, the equations were checked and suited to the configuration and confrontation was established between the test data and the computed results. The major merit of this examination is the characterization of the jets' interference effects in addition to the jet blockage effects. A more extended work conducted by Xiao [1992] concerned single, double and triple jets in a confined crossflow with constant boundary conditions for the jets and the duct flow. In the double and triple jets system, the centre-to-centre distances between the jets were 0.68 m and 0.20 m respectively. The blockage effect and the recirculation of the mainstream were found to be weaker for a system with a larger jet spacing and stronger for a system with a higher number of jets. Measurements of the jet velocity along the jet centerline of the multiple jet system were obtained, and the decay in the velocity of the upstream jet was found to be more rapid compared to the downstream jet in the tandem array. The latest work that followed this extended comparison for the twin jet configuration to the single and multiple jet cases was numerically carried out by Maidi et al. [2008] but on jets with a square exit section issuing normally. Here too single, double and triple jets configurations were considered for a jet to cross-flow velocity ratio of 2.5 and a Reynolds number of 225, based on the free-stream quantities and the jet width. The main results of this study consist in the strong dependence on the jet-to-jet edge distance of the merging process relative to two counter-rotating vortex pairs (CRVP) developed in the twin jets' configurations.

We see then that too little work was dedicated exclusively to the tandem jets in crossflow. Two scarce papers were however found in the literature. The first was carried out numerically by Ohanian et al. [2001] and handled two planer jets under a variable injection ratio and a variable jet spacing. They authors could mainly show the vanishing of the jets' coupling for the highest spacing (3 diameters) and the augmentation of the throw distance in the crossflow beyond the wall boundary layer thickness before finally tilting under the other spacing conditions and a rising exhaust momentum of the downstream jet above the free stream and upstream jet velocities. The second twin inline jets in crossflow examination was performed by Radhouane et al. [2009] under a variable initial streamwise inclination angle and tended to examine the heat and mass transfer generated by the different flows' interaction. We deduce from the above-mentioned references that too little work was dedicated to the temperature distribution in spite of the great relevance of the question especially under the incessant need for better efficiencies in most of the already mentioned applications. The need for increasing temperatures is however confronted with several serious drawbacks. In fact, in many of them, we are limited by technical constraints like the melting of the handled chambers' material. We may also be limited by environmental regulations as the ejection of too much heated jets in the atmosphere may engender acid rain or produce harmful molecular combinations especially in the case of industrial reactive fumes. To be able to provide viable solutions to such problems we propose to study precisely the impact of the variation of the gradient between the jets and the oncoming crossflow's temperatures. This impact will be explored mainly on the distribution of the temperature itself due to extremely high importance of this feature. For the matter we propose to describe the experimental side of this study that will provide us with reference for the validation of the numerical model. Then, we will explore numerically the temperature vertically as well as laterally in order to get a thorough idea about its three dimensional progression along the considered domain.

EXPERIMENTAL SET-UP

As announced before, experimental measurements are carried pout on a geometric replica. Its dimensions, the location of the jets nozzles, the orientation of the different present flows and the corresponding details are represented in figure 1.

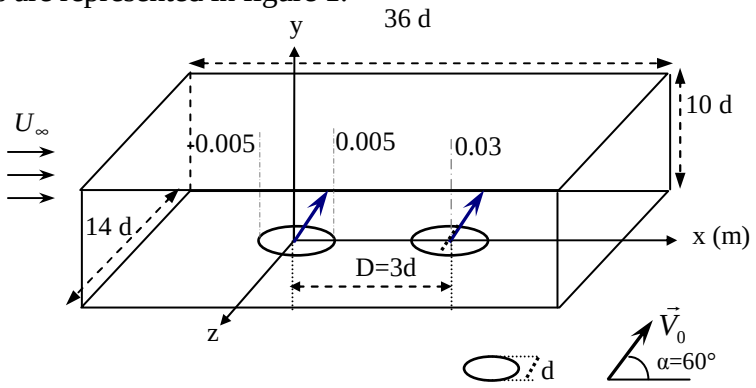

Figure 1. Geometry of the handled configuration

It is clear in the figure that the jets originated from cylindrical pipes finally result in elliptic cross section nozzles due to their razing at the level of the wind tunnel ground. We consequently diameters equal to d and d/sinα respectively in the lateral and longitudinal directions. Both jets and the crossflow are fed with air and the jets are first treated isothermally. For the need of the particle image velocimetry (PIV) technique and the images capturing the jets were seeded with glycerin particles whose diameter is approximately equivalent to 1 µm (the seeding density is approximately 30 particles per ml of pure jet fluid). As to the main air flow, it was seeded with oil droplets of approximately 0.8 µm diameter, and was introduced into the wind tunnel at the ambient temperature (T_∞). To characterize well and locate the different flow features, we chose a Cartesian coordinate system whose origin is located at the upstream jet nozzle center. This choice is motivated by the possible asymmetry of the resulting flowfield in spite of the symmetry of the geometry as stated in the literature by several authors like Smith et al.[1998], Muppidi et al.[2006], etc…
The different details concerning the PIV technique are available in the work of Radhouane et al. [2009] as they preceded the same in their former work.

NUMERICAL SIMULATION

Consideration is given to a steady, three dimensional, incompressible and turbulent flow. Having adopted a Cartesian coordinate system, the reigning Navier stokes equations become as follows:

$$\frac{\partial\left(\bar{\rho}\,\tilde{u}_i\right)}{\partial x_i} = 0 \tag{1}$$

$$\frac{\partial\left(\bar{\rho}\,\tilde{u}_i\,\tilde{u}_j\right)}{\partial x_j} = -\frac{\partial \bar{p}}{\partial x_i} + \frac{\partial}{\partial x_j}\left(\mu\frac{\partial \tilde{u}_i}{\partial x_j} - \overline{\rho\, u_i'' u_j''}\right) + \left(\bar{\rho}_\infty - \bar{\rho}\right) g\delta_{ij} \tag{2}$$

$$\frac{\partial\left(\bar{\rho}\,\tilde{u}_j\,\tilde{T}\right)}{\partial x_j}=\frac{\partial}{\partial x_j}\left[\left(\frac{\mu}{Pr}+\frac{\mu_t}{\sigma_t}\right)\frac{\partial\,\tilde{T}}{\partial x_j}\right] \tag{3}$$

$$\frac{\partial\left(\bar{\rho}\,\tilde{u}_j\,\tilde{f}\right)}{\partial x_j}=\frac{\partial}{\partial x_j}\left[\left(\frac{\mu}{Sc}+\frac{\mu_t}{\sigma_f}\right)\frac{\partial\,\tilde{f}}{\partial x_j}\right] \tag{4}$$

The introduction of the fluctuating functions and variables requires the use of a turbulence closure model. In the present work, we tested the ability of the *RSM* (Reynolds Stress Model) second-order model to fit well the experiments. Its introduction led to the resolution of the following equation:

$$\frac{\partial}{\partial x_k}(\bar{\rho}\tilde{u}_k\overline{u_i''u_j''})=\underbrace{\frac{\partial}{\partial x_k}}_{C_{ij}}\mu\underbrace{\frac{\partial}{\partial x_k}(\overline{u_i''u_j''})}_{D_{ij}^L}-\bar{\rho}\underbrace{\left[\overline{u_i''u_k''}\frac{\partial\tilde{u}_j}{\partial x_k}+\overline{u_j''u_k''}\frac{\partial\tilde{u}_i}{\partial x_k}\right]}_{P_{ij}}+D_{ij}^T+G_{ij}+\phi_{ij}+\varepsilon_{ij} \tag{5}$$

C_{ij} being the convective term, and D_{ij}^L, P_{ij}, D_{ij}^T, G_{ij}, ϕ_{ij}, ε_{ij}, respectively, the molecular diffusion, the stress production, the turbulent diffusion, the buoyancy production, the pressure strain and the dissipation rate of the turbulent kinetic energy [Schieste et al. 1993].

The equations of the turbulent kinetic energy (k) and of the dissipation rate of the kinetic energy (ε) associated with the second-order model are defined as follows:

$$\frac{\partial\left(\bar{\rho}\tilde{u}_j k\right)}{\partial x_j}=\frac{\partial}{\partial x_j}\left[\left(\mu+\frac{\mu_t}{\sigma_k}\right)\frac{\partial k}{\partial x_j}\right]+\frac{1}{2}\left(P_{ii}+G_{ii}\right)-\bar{\rho}\,\varepsilon \tag{6}$$

$$\frac{\partial\left(\bar{\rho}\tilde{u}_j\,\varepsilon\right)}{\partial x_j}=\frac{\partial}{\partial x_j}\left[\left(\mu+\frac{\mu_t}{\sigma_\varepsilon}\right)\frac{\partial\varepsilon}{\partial x_j}\right]+C_{\varepsilon1}\frac{1}{2}\left(P_{ii}+C_{\varepsilon3}G_{ii}\right)\frac{\varepsilon}{k}-C_{\varepsilon2}\bar{\rho}\frac{\varepsilon^2}{k} \tag{7}$$

For more information concerning the constants introduced in the different equations see reference [Mahjoub et al. 2003]

RESULTS AND DISCUSSION

The validation of our numerical replica is realized after confrontation of the calculated results to the experimental data. This confrontation is carried out on the vertical variation of both the longitudinal and the vertical velocity components. The corresponding profiles are taken for an injection ratio equivalent to R=1.29, a spacing of D=3d between the jet nozzles, an inclination of the jets equivalent to α=60° and at the center of the upstream jet nozzle location (figure 2).

The comparison of the calculated and measured results relatively to both components of the velocity results in a global satisfying agreement. The slight discrepancy detected in y=20 mm in the U velocity profiles are probably due to the transition from the first jet plume to the surrounding transverse flow. The matching of the vertical profiles is of a slight worse quality which may originate from a non uniformity in the jet seeding; even if the latter is regulated by a pumping system. We can then conclude that our numerical modeling is globally satisfying and models well the experimental configuration of the twin inclined jets issuing at α=60° within the oncoming crossflow.

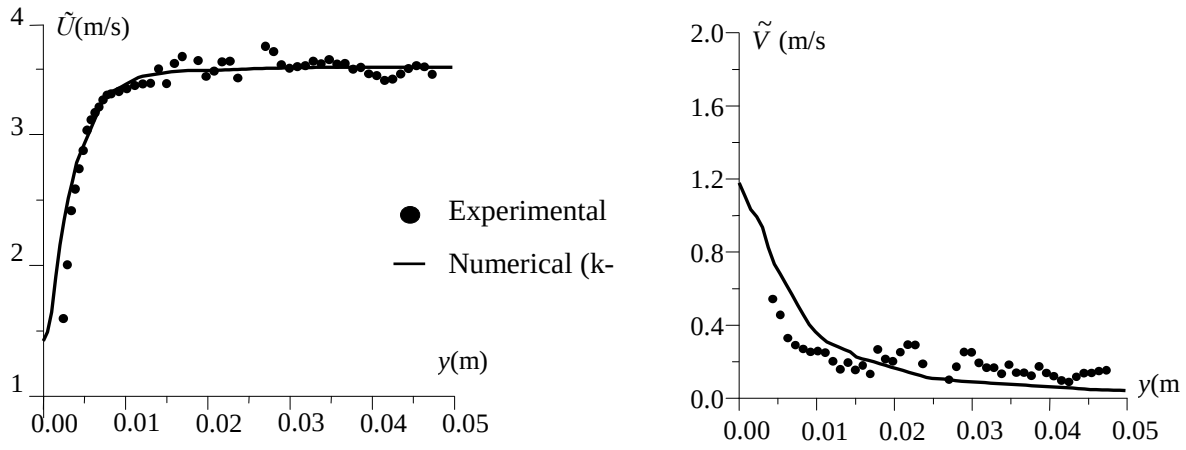

Figure 2 Validation f the numerical replica on longitudinal (a) and vertical (b) velocity components

We proceed now to the generalization of our simulated case by the introduction of the parameter to explore: the gradient between the jets and the crossflow temperatures. We are also going to introduce a non reactive fume within the emitted jets to approach better the reality; the fume being composed a follows: 76.9% N2, 20.9% CO2, 18% O2 and 0.4% SO2.

Now that defined the different imposed geometric, dynamic and mass conditions, we propose to represent the vertical distribution of the temperature itself under a variable gradient between the jets and the crossflow's temperatures (figure 3). The detailing of the temperature distribution will help us understand the consequences it brings on the behavior of the other governing features of the flowfield. The profiles will be plotted on the symmetry plane (z=0) and in the different characterizing regions of the domain (x=0, 15, 30 and 50 mm).

Herein, we have to precise that these locations are independent of the imposed conditions since they are relative only to the location of the jet nozzles. The domain is then divided as follows: within the first nozzle, between the jet columns, within the second nozzle and finally downstream the twin jets. The tested gradients are ΔT= 100K, 300K, 500K, 700K and 900K with reference to a constant crossflow's temperature equivalent to 303.15 K.

The augmentation of the temperature gradient is expressed within the first jet location (fig.3-a) by a higher initial value corresponding to the temperature imposed at the jet nozzle exit. When we flee the injection plate we note a similar global behavior consisting in a progressive decline leading to the total homogenization of the flowfield's temperature. This decline is consequently accompanied by a tighter declination slope due to the higher gradient considered. The total homogenization of the flowfield temperature finally occurs in the vicinity of y=14 mm.

The same thermal behavior is adopted within the downstream jet location with however the apparition of a second peak corresponding to the crossing of the rear jet's plume. The latter is naturally lower because the first jet has already been weakened by the oncoming crossing flow. The departure value is however the same as within the rear jet since we imposed the same injection conditions on both jets. The augmentation of the temperature gradient affects also the gradient existing between the registered peaks on a given profile. In fact, to the considered gradients ; that's to say ΔT= 100K, 300K, 500K, 700K and 900K corresponds respectively a temperature drop of approximately 35, 101, 250, 340 and 410K. That results in a drop rate equal to 0.35, 0.34, 0.5, 0.48, and 0.45 showing that the important changes occur under the first augmentations of the temperature gradients. Even if we keep the same trend in the augmentation of this parameter, we obtain a weaker variation between the two registered peaks. That leads us to suppose that the consequences of the temperature gradient increase won't be the same under the different tested values; this observation later will be checked later on the dynamic features.

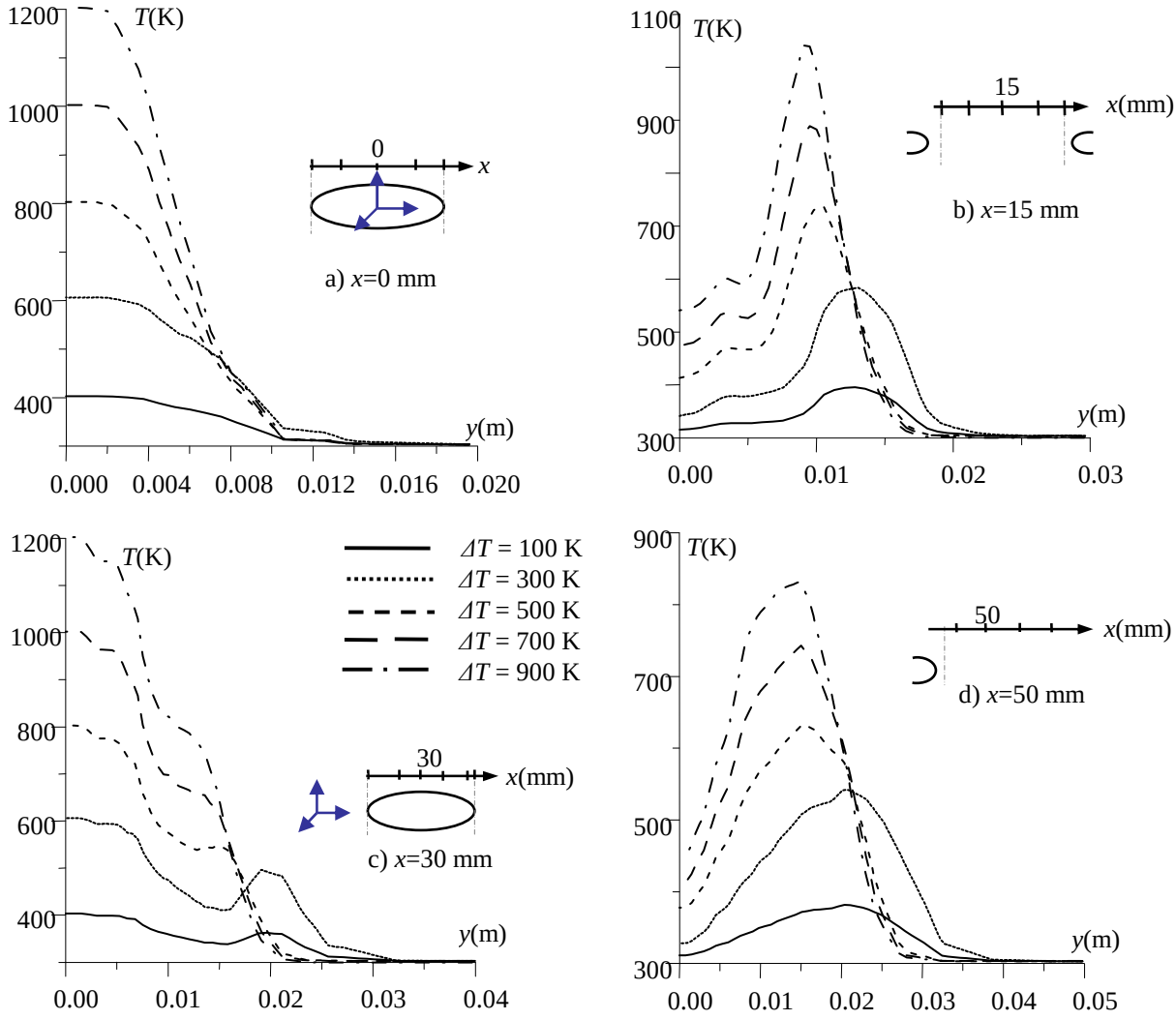

Figure 3 Influence of the variation of the temperature gradient on the vertical distribution of the temperature in the different characterizing zones of the domain

Within the jet nozzles (fig.3-b), the profiles start from different initial values even if we are always situated at the injection plate. This is also due to the augmentation of the temperature gradient. In fact, on one hand we kept the crossflow at the same temperature and the velocity ratio unchanged whereas on the other hand we increased the jets' temperature. These two assumptions allow the temperature plume of the rear jet to keep its thermal potential core longer and wider in the domain. Its presence is consequently perceived more significantly everywhere and particularly close to the injection plate. This impact is then optimum under the highest temperature gradient due to the wider extent of the corresponding plumes. In addition to this, we can also note the presence of an initial maximum that is rather a stage than a single peak more precisely under the first temperature gradients (ΔT=100 and 300K). As this gradient carries on rising, the registered peak rises. Nevertheless these maxima are not due to the crossing of the rear jet's extension but to the crossing of the flow trapped between the jet columns. The flow in this region is strongly affected by the jet columns; that's why its temperature increases when the jets are heated. Finally, we note that the decline slope of the temperature is slower under the two first gradients (100 and 300K) whereas it becomes tighter as this gradient increases; we even see that it becomes almost the same in the remaining cases; in the vicinity of the crossflow's temperature (T_∞=303.15K)

Downstream of the twin jets, the same behavior is reproduced with however some discrepancies. The temperature reaches one single peak whose value is weaker than within the jet nozzles. That's due to the fact that the jets; even combined; have already crossed the domain and then have lost some of their strength (their heat in this case). The second change concerns the width of the temperature profile since under all the considered cases we have wider thermal distributions; the decline slope is however maintained approximately the same as between the nozzles' jets.
We can then conclude that the augmentation of the gradient between the jets and the crossflow's temperatures widens the temperature profiles, increases the registered peaks and postpones the homogenization of the flowfield's' temperature due to the deeper and wider extant of the jet plumes.
The consideration of the lateral distribution of the temperature is as important as the vertical one in the way it provides a thorough idea about the three dimensionally of the problem. The same tested gradients were considered and their impact was evaluated on the distribution of the temperature within the already defined longitudinal locations. We also considered three different vertical levels with reference to the injection plate in order to sweep away the majority of the interesting zones contained within the domain. The farthest vertical position explored is y=8 mm just because of the insignificance of the variations and even their vanishing beyond of this location. We begin in figure 4 with what occurs within the jet nozzles' locations; what happens elsewhere will be treated later.
A primer global observation of the different plotted profiles shows a quasi symmetric behavior of the temperature. They are however not Gaussian because close to the injection wall the maximum is reached during a whole stage and on the following profiles several disturbances appear and the asymmetry is comforted. In fact, at y=2 mm, the closest plane (fig. 4-I-a), we are too close to the jet nozzles' exit section. The jets are then just emitted and have not accused the influence of the oncoming crossflow. The thermal potential core of the jets are then still intact which justifies the persistence of the maximum temperature value along the jets' little diameter (≈10 mm). Of course the persistence of this maximum does not occur similarly under the different tested gradients since the less heated jets adopt the most regular maximum stage before declining on both sides of the symmetry plane. This is due to the approximate equivalence of the thermal forces relatively to the emitted jets and the mainstream (the gradients is only 100 K). This induces a progressive dispersion of the thermal potential core of the rear jet and the longer persistence of its maximum. As the jets are heated further, their density is decreased which lightens their corresponding plumes and accelerates their crossing of the environing flow. This quicker expanding through the domain is precisely at the origin of the quicker reduction of their initial temperature maximum. The latter is detected on the plotted profiles through the progressive registration of a single peak in stead of a whole stage and in the adoption of a more sudden decreasing slope on both sides of the symmetry plane (z=0) which gives a more rounded allure to the profiles. The augmentation of the imposed gradients also results in a quicker peripheral homogenization of the resulting flowfield temperature. In fact, even if the final homogenization takes place approximately at the same location on the first vertical plane, it is however attained following a greater decline slope (z=± 12 mm). Nevertheless, we can not talk about perfect Gaussian profiles because the final homogenization takes place effectively at different locations on both sides of the symmetry plane (z=-13 mm and z=15 mm). The detected flow asymmetry is very interesting due to its prior contradiction with the geometry symmetry. We propose to check it later on the remaining temperature and other features' profiles. For now, we propose to move farther from the jet nozzle exits to consider the changes brought by the temperature ratio on the corresponding profiles. These changes are in fact more spectacular like the apparition of a lateral like peak in the vicinity of z= -7 mm and the disturbance present on the declining slope at z=6 mm. These two singularities may actually result from the gradient between the jets and the mainstream pressures as proposed by Muppidi et al. [2005]. A further explanation to the asymmetry was given by Su et al. [2004] and was approved by Muppidi et al. [2006] and was even generalized for the instantaneous and mean flows.

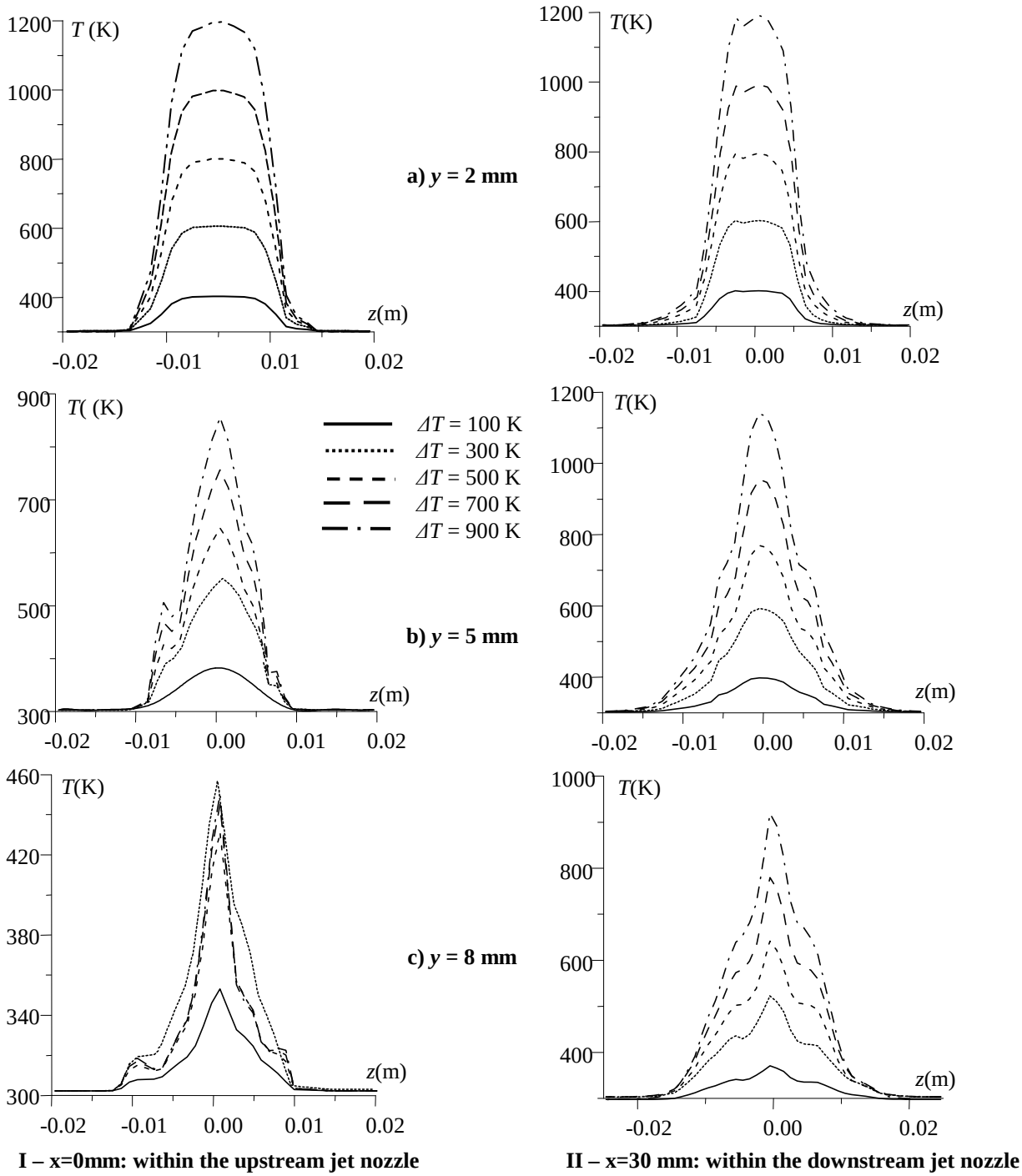

Figure 4 Influence of the variation of the temperature gradient on the lateral distribution of the temperature at different vertical levels within the twin jet nozzles

This explanation supposes it to originate from the interaction itself with the mainstream propelling the jets towards the developed wake region. From far downstream, this orientation seems to lead the jets rather to the peripheral sides and not to the central axis (z=0). A further factor is likely to reinforce the symmetry according to Su et al. [2004] and consists in the higher momentum on the interface face with the jets.

Apart from these singularities, the same observations are maintained concerning the impact of the temperature gradient. Its augmentation still engenders a higher reached peak, generates a thinner

profile and results in a quicker declining slope: the heated jets are quicker to disperse and then quicker to loose their initial "heat potential". With reference to the previous plane, the final homogenization occurs earlier: at z≈±10 mm in stead of z≈±14 mm and that under all the tested cases. This is due to the already began dispersion process of the initial jets' temperature whatever the imposed gradient is. At the highest plane (fig. 4-I-c), the profiles are thinned further always due to the advanced progression of the dispersion process. The latter progressed so much that we observe even profiles with a needle like allure particularly under the highest temperature gradient. The asymmetry as predicted is further reinforced by the adoption of the profiles different declining slopes and we even note a further disturbance at the vicinity of z=-10 mm.

When move to the second jet location (fig. 4-II), we observe approximately the same behavior with however some discrepancies. For example, the final homogenization of the resulting flowfield temperature does no longer occur simultaneously under the different tested cases. It occurs earlier when the jets are less heated and that at the different examined vertical levels. The profiles are however still narrower under the highest gradients which is reasonable due to the always faster dispersion of the jet initial temperature. The change in the homogenization moment is also due to this reason as the quicker expansion of the second jet takes place also in the lateral direction as shown in figure 5 where we represented the temperature contours. In this way, the surrounding flow is heated further as the imposed temperature gradient rises. Its cooling by the oncoming crossflow will consequently take more time and this process is expressed on the profiles through a more progressive final decline. On these same profiles we said that the declining slopes became more regular with reference to the upstream jet location; they however contain a ghost of stages at the vicinity of z≈±5 mm. The asymmetry is present here through the different emplacement of the registered stages as it occurs effectively between -6 and -3 mm at the left side and between 5 and 7 mm on the right one. Generally speaking, the asymmetry of the potted distributions is less pronounced then in the upstream jet location due to the more "strong" confrontation between the rear jet and the crossing flow. This is due to its prior location which enables it to undergo its entire flattening and tilting effects. The downstream jet is on the contrary prevented from a direct interaction with the main flow thanks to the shielding effect provided by rear one. The perturbations are consequently significantly reduced which allows the temperature profiles to keep a regular allure.

The already discussed stages appeared clearly only under the three highest temperature gradients at the y=5 mm vertical level. They however were further comforted and generalized on the farthest plane (y=8 mm). These observations are better shown on the temperature contours especially that we added the distribution on a further higher plane located at y=12 mm (fig. 5). We can that these stages are actually engendered by the lateral expansion of the rear jet plume that joins the one relative to the just emitted downstream jet. A more significant region is consequently heated on both sides of the potential core of the second jet which results in wider stages on the temperature profiles during the homogenization process. Theses stages however don't signify a later final homogenization of the resulting flowfield as we the heated flow always disperses more rapidly which is the case if we pay attention to the position at which the flow finally gains the crossflow temperature: approximately z=±13, 15 and 20 mm under respectively y=2, 5 and 8 mm.

The final remark concerns the rate of reduction of the registered peaks that is closely related to the imposed temperature gradient. This rate is respectively equivalent to 6.67, 5.26, 3.75, 3.33 and 0% between the first and second plane values and 17.85, 17.89, 15.58, 11.86 and 12.5% when progressing from the second to the highest plane.

Now that we examined the lateral behavior of the temperature within the jet nozzles' locations, we propose to move to the remaining characterizing zones that are extremely interesting due to the striking phenomena they enclose.

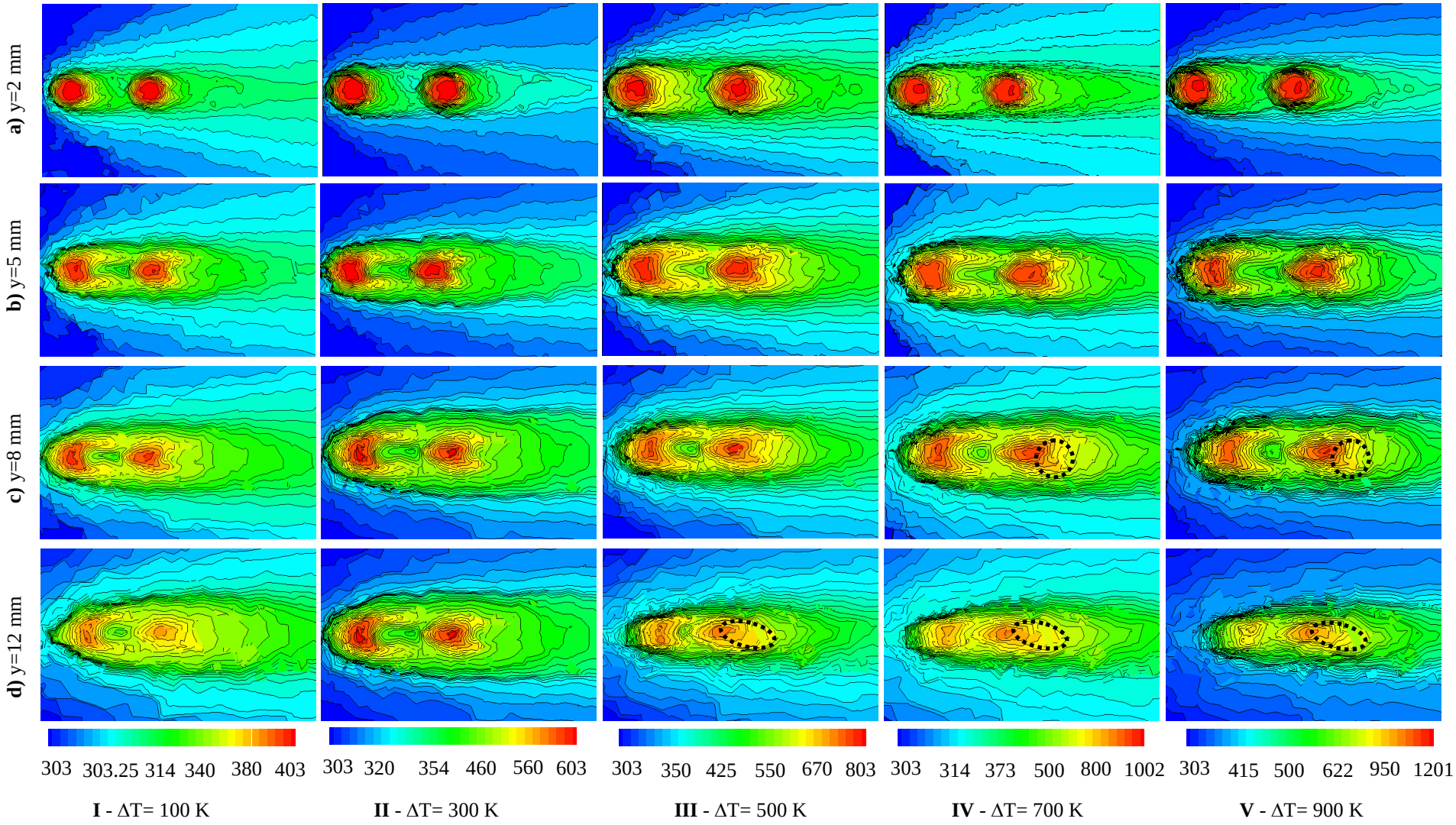

Figure 5. Impact of the temperature gradient on the lateral expansion of the temperature cartographies at different vertical levels

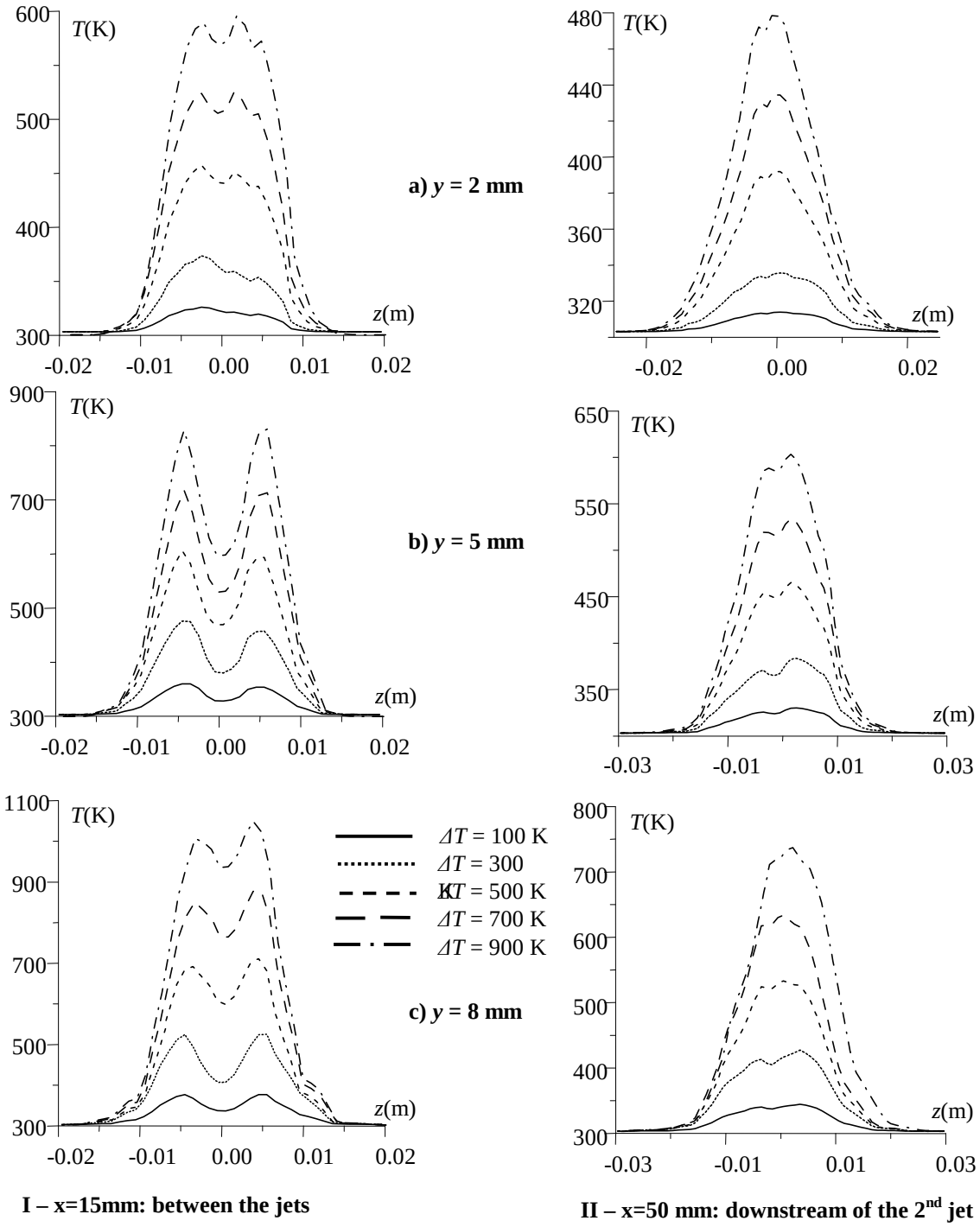

Figure 6 Influence of the variation of the temperature gradient on the lateral distribution of the temperature at different vertical levels between and downstream of the jet nozzles

These phenomena consist mainly in the development of a wake region downstream of both of the jets and this region is more singular downstream of the upstream one because of its confinement between the emitted jet columns as shown on the already observed temperature contours (fig. 5). We propose then to begin with the profiles plotted in this region at the same different vertical levels (fig. 6-I). The change in the temperature behavior appears immediately close to the injection cross section exit (y=2 mm) as we longer assist to the registration of a single peak but two. Their corresponding maxima reach different values that are progressively approached as the temperature

gradient increases. The symmetry of the profiles is not realized as far since a further perturbation develops on the temperature distributions at the vicinity of z=5 mm departing from a temperature gradient equal to 300 K.
Though it exists, the asymmetry is not very clear on the temperature contours; it becomes only at the highest planes (y=8 and 12 mm) as shown within the encircled zones (fig. 5-c and d). When we flee further the injection plate, the jets' thermal potential cores are more rapidly dispersed but they are confronted with the wake region that is trapped between the jet columns. This process results in a more significant dividing of the initial upstream jet plume as the wake region is characterized by a lower temperature. A wider space develops consequently between the registered temperature peaks. Here in the contrary the symmetry of the profiles is improved. That may result from our farther location from the injection plate and then from the main interaction zone. This observation is however no longer true when carry on going farther from the injection plate since the augmentation of the temperature gradient when we are located at the highest plane brings a further asymmetry leading to higher peaks on the right side (positive z coordinates).
Downstream of the twin jet nozzles, we find back a single peak and a general decline of the temperature with reference with what happens between the jet nozzles. We however observe a slight decline on the registered peaks that is certainly going to disappear a little farther. Its origin existence comes from the flattening of the combined jet plumes by the crossing flow. This flattening is as previously said more pronounced under the highest gradients due to their weaker density and then to their resistance towards the constant temperature of the mainstream (fig 5-IV and V c and d). As we move farther from the injection plate, we observe the progressive establishment of a more pronounced asymmetry and even a sweeping of the temperature profiles towards the positive coordinates side. The persistence of the peak dividing will certainly take over if we move further downstream; when the jets completely combine and result in a single plume.

CONCLUSION

The present study considered both experimentally and numerically twin inclined elliptic jets in crossflow. The jets were inclined with a 60° angle and their corresponding nozzle centers were spaced with a distance equivalent to three diameters. We mainly focused on the consequences of the variation of the gradient between the jets and the crossflow temperature in order to evaluate the impact of this parameter on resulting flowfield temperature both vertically and laterally. The augmentation of this parameter proved to widen the temperature profiles, to increase the registered peaks and to postpone the final homogenization of the flowfield's temperature due to the deeper and wider extent of the jet plumes.
Heating the emitted jets further also allowed them to flee the injection plate more rapidly but in the same time to be flattened more significantly by the oncoming flow due to their weaker density. This phenomenon generated the in most of the time the registration of twin peaks in stead of a single one because of the wake regions that developed downstream of each of the nozzles and represented a king of obstacle in front of the free jets progression.

REFERENCES

Di Micco, R.G., Fabris, D. Disimile, P.J. [1990], The effect of constructive and destructive interface on the downstream development of twin jets in a crossflow. Part1: destructive interference of laterally spaced jets. *AIAA-90-1623*

Di Micco, R.G., Fabris, D., Disimile, P.J., [1990] The effect of constructive and destructive interface on the downstream development of twin jets in a crossflow. Part2: Interference effects of angularly displaced jets. *AIAA, SAE: 26th ASME, and ASEE, Joint Propulsion Conference*, Orlando, FL, 12 p

Kolar, V., Savory, E., Takao H., Todoroki, T., Okamoto, S., Toy, N. [2006],Vorticity and Circulation Aspects of Twin Jets in Cross-Flow for an Oblique Nozzle Arrangement, *Proceedings of the Institution of Mechanical Engineers, Part G: Journal of Aerospace Engineering*, 220(4), pp.247-252

Kolar, V., Savory, E. [2007], Dominant flow features of twin jets and plumes in crossflow, *Journal of Wind Engineering and Industrial Aerodynamics*, 95, pp. 1199–1215

Mahjoub Said N., Mhiri, H., Golli, S., Le Palec, G., Bournot, P. [2003], Three Dimensional Numerical Calculations of a Jet in An External Crossflow: Application to Pollutant Dispersion, ASME *J. of heat transfer*, 125

Maidi, M., Yao, Y. [2008], Numerical Visualization of Vortex Flow Behavior in Square Jets in Cross-Flow, *Journal of visualization*, 11(4), pp. 319-327

Moore, C.L.; Schetz, J.A. [1985], Effects of non-uniform velocity profiles on dual jets in a crossflow, *18th Conference of Fluid Dynamics, Plasma dynamics and Lasers*, American Institute of Aeronautics and Astronautics, Cincinnati, OH; United States; 10 pp

Muppidi, S., Mahesh, K. [2005], Study of trajectories of jets in crossflow using direct numerical simulations, J. Fluid. Mech

Muppidi, S., Mahesh, K. [2006], Two-dimensional model problem to explain counter-rotating vortex pair formation in a transverse jet, *Physics of Fluids J*. 18(8)

Ohanian, T., Rahai, H.R. [2001], Numerical investigations of multi turbulent jets in a crossflow, *AIAA 2001-1049*.

Radhouane, A., Mahjoub Saïd, N., Mhiri, H., Le Palec, G., Bournot, P. [2009], Impact of the initial streamwise inclination of a double jet emitted within a cool crossflow on its temperature field and pollutants dispersion, *Heat and Mass Transfer*, 45(6), pp. 805-823

Schieste, R., Launder B.E. [1993], Modélisation et Simulation des Ecoulements Turbulents, Hermès, Paris, France

Smith S.H, Mungal M.G. [1998], Mixing, structure and scaling of the jet in crossflow. *J Fluid Mech* 357, pp. 83-122

Su, L.K., Mungal, M.G. [2004], Simultaneous measurement of scalar and velocity field evolution in turbulent crossflowing Jets. J. Fluid Mech. 513: 1-45.

Toy, N., Disimile, P.J., Savory, F., McCusker, S. [1992], The development of the interface region between twin circular jets and a normal crossflow, *13th Symposium on Turbulence*, Univ. of Missouri-Rolla; United states

Xiao, D. [1992], Experimental and computational investigation of multiple jets in a duct crossflow *Ph.D. thesis*, Dept. of Chemical Engineering, Queen's University, Kingston, Ontario, Canada

Ziegler, H., Wooler, P.T. [1970], Multiple Jets Exhausted into a Crossflow, *Journal of Aircrafl*, 8(6), pp. 414-420.

Ziegler, H., Wooler, P.T. [1973], Analysis of stratified and closely spaced jets exhausting into a crossflow, National Aeronautics and space Administration, Washington, D.C.